Electronic Supplementary Material (ESI) for Journal of Materials Chemistry A.
This journal is © The Royal Society of Chemistry 2018

Supporting Information

Solid-phase hydrogen in magnesium-carbon composite for efficient hydrogenation of carbon disulfide

Haipeng Chen,[ab] *Zongying Han,*[b] *Xun Feng,*[a] *Pei Liu,*[b] *Jinqiang Liu,*[a] *Guilong Liu,*[a] *Weiwei Yuan,*[a] *Tianjiao Ren*[a] *and Shixue Zhou**[b]

[a] College of Chemistry and Chemical Engineering, Henan Key Laboratory of Function-Oriented Porous Materials, Luoyang Normal University, Luoyang 471934, China

[b] College of Chemical and Environmental Engineering, State Key Laboratory of Mining Disaster Prevention and Control Co-founded by Shandong Province and the Ministry of Science and Technology, Shandong University of Science and Technology, Qingdao 266590, China

Corresponding author: Tel: +86 532 86057857. E-mail: zhoushixue66@163.com (S.X. Zhou)

Preparation of pure MgH_2: Mg powders (>99.0%, Tianjin Ruijinte Chemical Company) were sieved first and those smaller than 0.074 mm were used for preparation of pure MgH_2. The hydriding of Mg powders for pure MgH_2 preparation was carried out on an isothermal adsorption instrument (PCTPro-2000, Setaram) by using temperature 400 ^{o}C and H_2 pressure 4.0 MPa.

Preparation of carbon additive: Carbon additive was prepared by demineralization and carbonization of anthracite (Rujigou Mine, China). Demineralization was first mixing anthracite (10.0 g) and NaOH (12.0 g) in a stainless-steel vessel and heating at 400 ^{o}C for 1.5 h. The mixture was then cooled down to room temperature and rinsed with deionized water. After that, the anthracite was soaked with hydrochloric acid (120 mL, 57 wt% in water, J&K) and rinsed with deionized water after heated at 80 ^{o}C in water bath for 4.0 h. Carbonization of anthracite was carried out in a crucible at 900 ^{o}C for 1.0 h under argon atmosphere. When the furnace was naturally cooled to room temperature, the carbon additive was obtained.

Transition states calculation: Transition states (TS) were calculated by using the complete LST/QST method. Before calculation, adsorbent atoms were set as “Hessian atoms”. Frequency calculations for initial state (IS) and final state (FS) were first calculated to confirm that they didn’t have imaginary frequencies. During calculation, electronic Hamiltonian setting was the same to that of geometry optimization. TS optimization was used to confirm the right imaginary frequency, and TS confirmation was used to further confirm the TS.

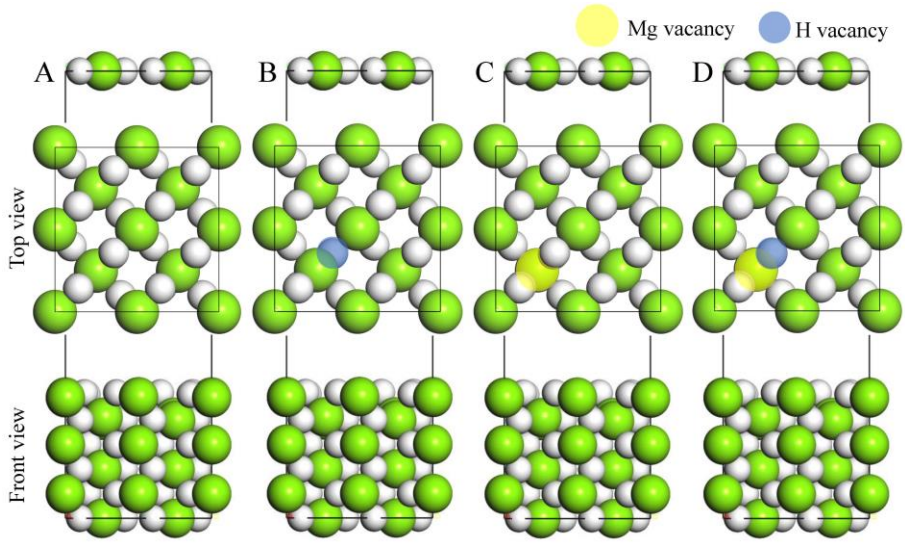

Fig. S1 Schematic illustration for A) clean $MgH_2(001)$, B) clean $MgH_2(001)$ after offering a H atom, C) defective $MgH_2(001)$, and D) defective $MgH_2(001)$ after offering a H atom.

The energy required for offering a H atom can be calculated as follows:

$$E_{required} = E_{total\text{-}H} + E_H - E_{total} \quad \text{(S1)}$$

where $E_{required}$ is the energy required for offering a H atom from clean or defective $MgH_2(001)$; $E_{total\text{-}H}$ is the total energy of clean or defective $MgH_2(001)$ after offering a H atom; E_H is the energy of a H atom; E_{total} is the total energy of the clean or defective $MgH_2(001)$.

Table S1 Calculation results for the energy required of offering a H atom from clean and defective $MgH_2(001)$

Surface	$E_{total\text{-}H}$ (Ha)	E_H (Ha)	E_{total} (Ha)	$E_{required}$ (eV)
Clean $MgH_2(001)$	-4827.5710	-0.4998	-4828.1964	3.42
Defective $MgH_2(001)$	-4627.4426	-0.4998	-4627.9716	0.79

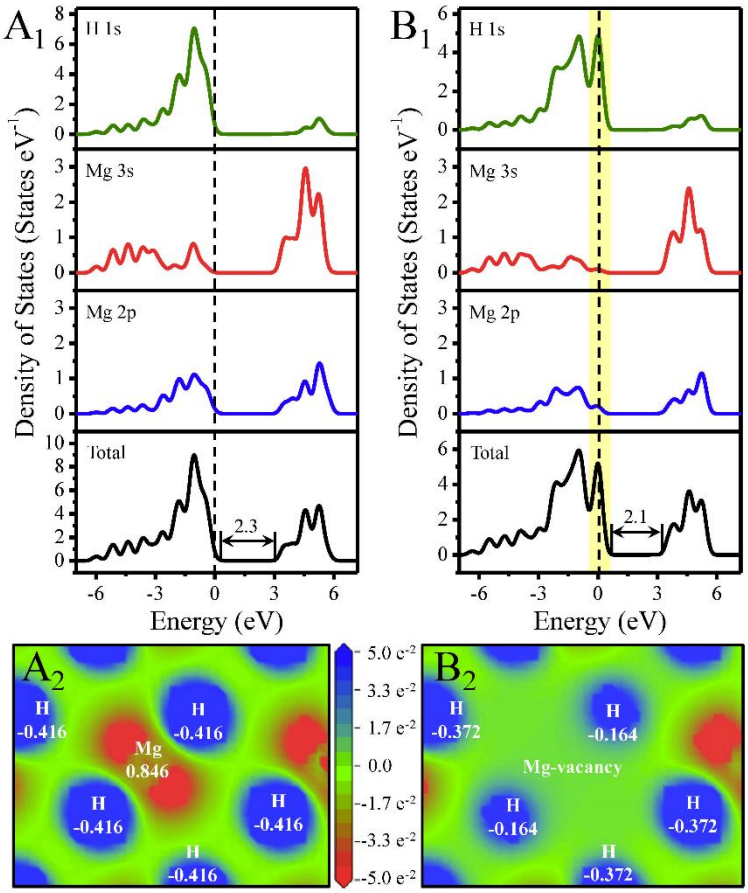

Fig. S2 A_1,B_1) Density of states (DOS), and A_2,B_2) deformation charge density for CS_2 molecules adsorbing on MgH_2(001), where A,B) represent for clean surface and defective surface, respectively. From calculation, the band gap of MgH_2(001) is 2.3 eV, and reduces to 2.1 eV when introducing Mg_{vac} defect. Moreover, from Mulliken population analysis, the H atoms those closing to Mg_{vac} defect can loss some electrons, suggesting that localization degree of electrons on MgH_2 surface reduces and electrons transfer increases by introducing Mg_{vac} defect.

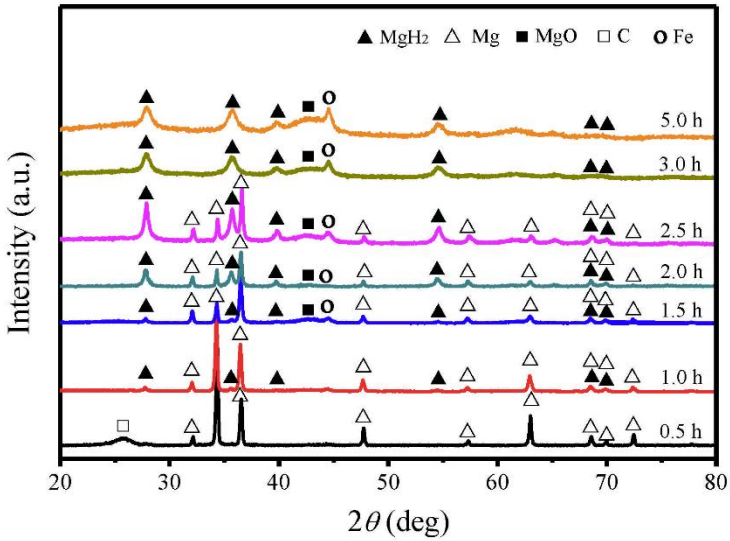

Fig. S3 XRD patterns of Mg-carbon hydrogen storage composite from 0.5-5.0 h of ball milling under 1.0 MPa H_2.

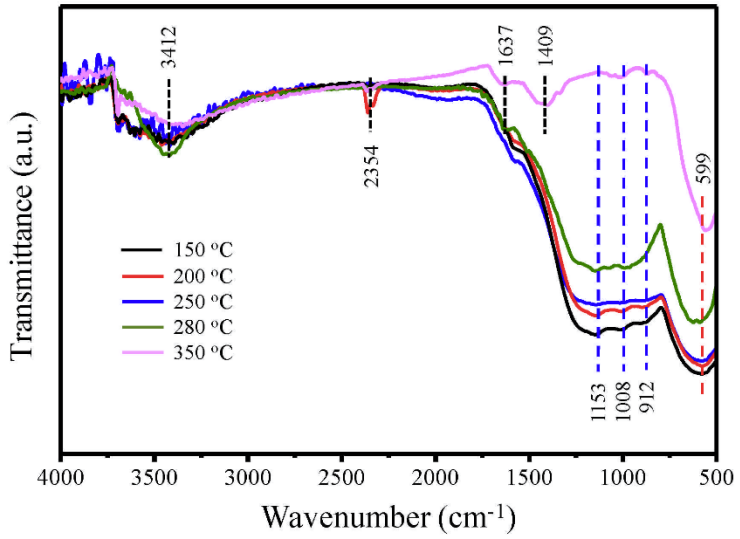

Fig. S4 FT-IR spectra for Mg-carbon hydrogen storage composite (2.5 h of ball milling, 1.0 MPa H_2) after heating at temperatures 150-350 °C. With the increase of temperature, absorption peaks for aromatic C-H at 599 cm^{-1} and in the range 912-1153 cm^{-1} become weak, while absorption peaks for aromatic C=C at 1409 and 1637 cm^{-1} become strong, suggesting that hydrogen can combine with carbon by C-H dangling bonds. From dehydriding measurement, the total hydrogen amount of the composite is 5.6 wt%, and the amount of hydrogen stored by carbon should be small, because it can only store 0.4 wt% of hydrogen even for 5.0 h of ball milling without the presence of Mg.

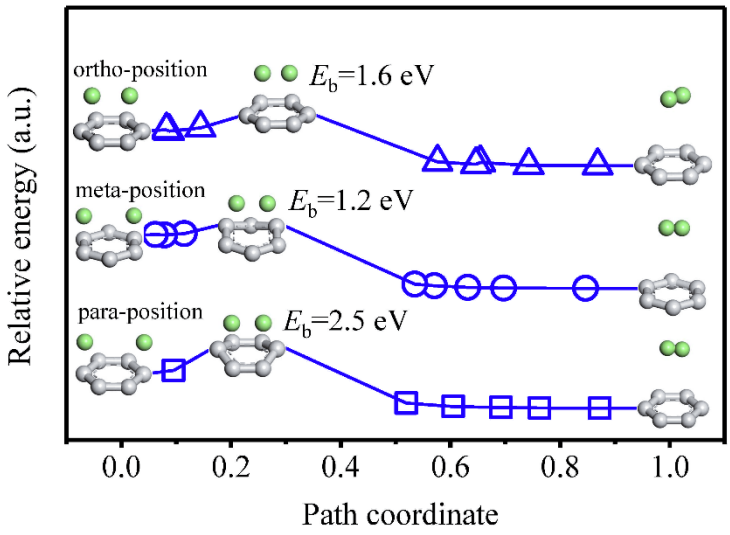

Fig. S5 Minimum energy paths (MEPs) for dehydriding from carbon basal plane. There are three sites, i.e. top site, hollow site and bridge site, for hydrogen adsorption on carbon basal plane. Theoretical calculations show that the energy barrier for H_2 molecule desorption from carbon is 1.8 eV in average. Although H atoms can be captured by carbon, the attractive force is weak, and hydrogen can easily desorb from carbon basal plane.

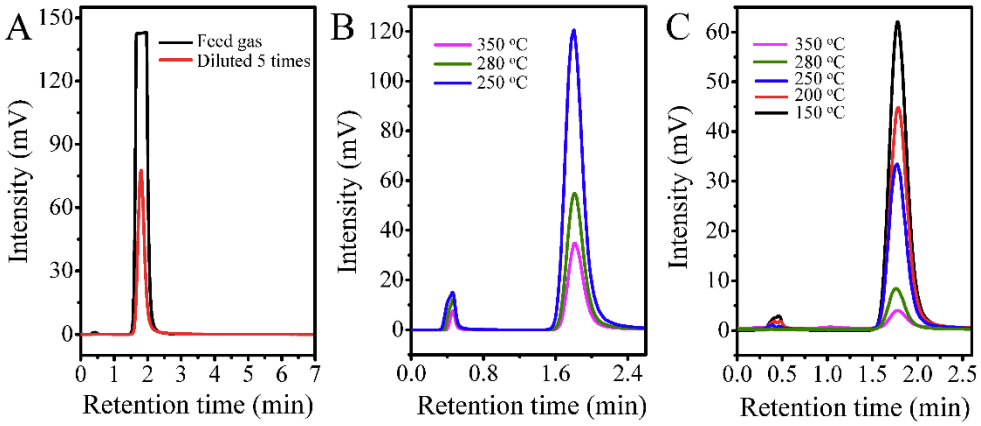

Fig. S6 A) Chromatogram of feed gas. Chromatogram for CS_2 in outlet gases after 300 min hydrogenation by B) pure MgH_2 and C) Mg-carbon hydrogen storage composite. Compared to pure MgH_2, Mg-carbon hydrogen storage composite has a higher performance for CS_2 hydrogenation due to its defective structure.

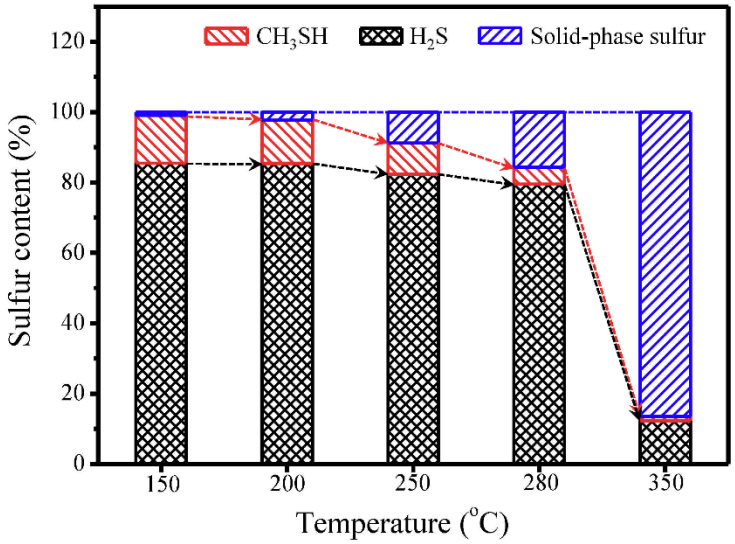

Fig. S7 Distribution for sulfur from CS_2 hydrogenation by Mg-carbon hydrogen storage composite at temperatures 150-350 ºC. Results show that hydrogenation temperature plays a critical role in product composition. Gaseous products are dominant at low temperatures, while solid products are dominant at high temperatures.

Table S2 Equilibrium lattice constants and cohesive energy (E_{coh}) of MgH_2.

Parameter	This calculation	Experimental[1,2]	Other calculation[3]
a (nm)	0.4514	0.4501	0.4495
c (nm)	0.3019	0.3010	0.3006
c/a	0.6688	0.6687	0.6687
E_{coh} (eV)	6.6186	-	6.70

As shown in **Table S2**, the value of *c*/*a* from this calculation is 0.6688, which is in good agreement with the corresponding experimental value 0.6687[1,2] and previous theoretical value 0.6687.[3] The calculated cohesive energy is E_{coh} = 6.6186 eV, which is similar to other calculation result E_{coh} = 6.70 eV.[3]

Table S3 Results for convergence with respect *k*-points.

k-points	E_{total} (Ha)	*k*-points	E_{total} (Ha)	*k*-points	E_{total} (Ha)	*k*-points	E_{total} (Ha)	*k*-points	E_{total} (Ha)
(1×1×1)	-4828.1633030	-	-	-	-	-	-	-	-
(2×1×1)	-4828.1813855	(2×2×1)	-4828.1966106	-	-	-	-	-	-
(3×1×1)	-4828.1812394	(3×2×1)	-4828.1964934	(3×3×1)	-4828.1963804	-	-	-	-
(4×1×1)	-4828.1812427	(4×2×1)	-4828.1964949	(4×3×1)	-4828.1963822	(4×4×1)	-4828.1963840	-	-
(5×1×1)	-4828.1812427	(5×2×1)	-4828.1964949	(5×3×1)	-4828.1963822	(5×4×1)	-4828.1963839	(5×5×1)	-4828.1963839

For supercell calculations, the *k*-points used was 3 × 3 × 1, which is in line with the calculation from H. Wang, et al.[4] The convergence with respect *k*-points was checked, as shown in **Table S3**, the total energy for *k*-points 3 × 3 × 1 is -4828.1963804 Ha, and that for *k*-points 4 × 4 × 1 is -4828.1963840 Ha. The small difference (0.0000036 Ha) indicates that *k*-points 3 × 3 × 1 is reliable for calculations.

Table S4 Results for Rietveld refinement and crystallite size calculation based on XRD data of the composite from reactive ball-milling.

Milling time (h)	Crystal phase	Unit cell parameters (nm)			Crystallite size (nm)	Abundance (wt%)	Refinement R_{wp} (%)
		a	*b*	*c*			
1.5	MgH_2	0.4487	0.4487	0.3001	10.6	10.36	6.21
	Mg	0.3208	0.3208	0.5210	55.3	82.04	
	MgO	0.4247	0.4247	0.4247	12.3	3.14	
	Fe	0.2951	0.2951	0.2951	15.1	4.46	
2.0	MgH_2	0.4486	0.4486	0.3003	25.3	38.43	5.79
	Mg	0.3210	0.3210	0.5224	47.3	49.33	
	MgO	0.4236	0.4236	0.4236	13.3	8.68	
	Fe	0.2948	0.2948	0.2948	15.6	3.56	
2.5	MgH_2	0.4497	0.4497	0.3005	32.6	41.06	6.06
	Mg	0.3212	0.3212	0.5212	45.7	22.03	
	MgO	0.4257	0.4257	0.4257	14.3	34.58	
	Fe	0.2950	0.2950	0.2950	16.0	2.33	
3.0	MgH_2	0.4502	0.4502	0.3012	21.8	72.65	5.83
	MgO	0.4218	0.4218	0.4218	15.5	25.13	
	Fe	0.2876	0.2876	0.2876	14.8	2.22	
5.0	MgH_2	0.4496	0.4496	0.3005	20.6	51.28	5.47
	MgO	0.4234	0.4234	0.4234	14.5	43.06	
	Fe	0.2953	0.2953	0.2953	15.3	5.66	

Crystallite sizes, i.e. the vertical direction dimensions of crystal planes, are calculated by the Scherrer equation as follows:

$$L_c = K\lambda/\beta \cdot \cos\theta \tag{S2}$$

where L_c is the crystallite size, nm; K is the dimensionless shape factor, K = 0.94; λ is the X-ray wavelength, λ = 0.154056 nm; β is the full width of diffraction peak at half maximum intensity (FWHM), radian; and θ is the Bragg angle, degree. Herein, Mg($10\bar{1}1$), MgH_2(101), MgO(200) and Fe(110) at 2θ = 36.62°, 35.74°, 42.92° and 44.67°, respectively, are adopted for crystallite size calculations.

Table S5 Kinetic equations and their goodness of fitting for carbon, MgH_2 and composite. From fitting, the best kinetic models for carbon, MgH_2 and composite are JMA 2D, JMA 3D and CV 3D civ, respectively.

Kinetic model	Equation $f(\alpha)$	Kinetic model description	Goodness of fitting, Adj. R^2		
			Carbon	MgH_2	Composite
JMA 2D	$2(1-\alpha)[-\ln(1-\alpha)]^{1/2}$	Two-dimensional growth of existing nuclei with constant interface rate.	0.965	0.942	0.945
JMA 3D	$3(1-\alpha)[-\ln(1-\alpha)]^{2/3}$	Random bulk nucleation/surface and three-dimensional growth with constant interface velocity.	0.920	0.960	0.946
CV 2D	$2(1-\alpha)^{1/2}$	Contracting volume, two-dimensional growth with constant interface rate.	0.937	0.911	0.923
CV 3D civ	$3(1-\alpha)^{2/3}$	Contracting volume, three-dimensional growth with constant interface rate.	0.906	0.904	0.981
CV 3D div	$(3/2)[(1-\alpha)^{-1/3}-1]^{-1}$	Contracting volume, three-dimensional growth diffusion controlled with decreasing interface velocity.	0.875	0.800	0.867

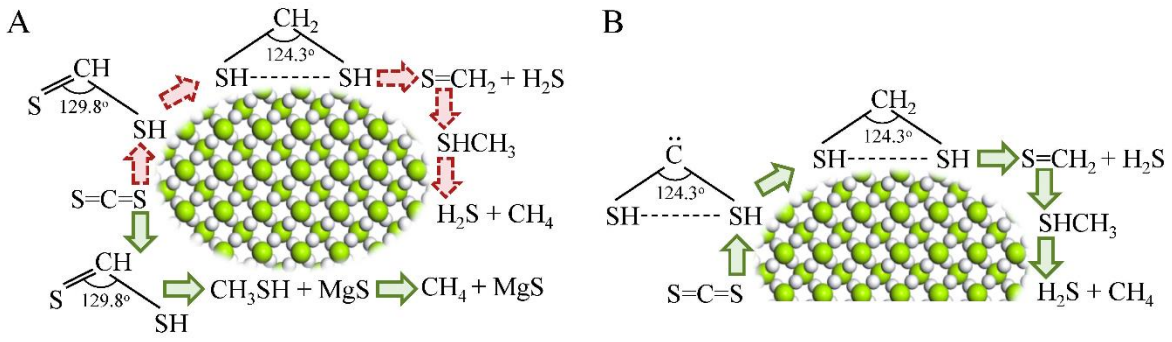

Scheme S1 Schematic illustration for reaction paths of CS_2 hydrogenation by A) vertical and B) horizontal path on MgH_2 surface. Comparing with the two cases, the horizontal path is the main path for CS_2 hydrogenation because it can benefit the adsorption of CS_2 molecules and the formation of intermediate products. When high temperature reduces the role of adsorption in hydrogenation, the vertical path becomes obvious, by which Mg crystals from MgH_2 decomposition can react with sulfur to form MgS, verifying experimental results.

References:

[1] M. Bortz, B. Bertheville, G. Bottger and K. Yvon, *J. Alloys Compd.*, 1999, 287, L4-L6.

[2] G. Wu, J. Zhang, Q. Li, Y. Wu, K. Chou and X. Bao, *Comp. Mater. Sci.*, 2010, 49, 5144.

[3] Z. Hou, *J Power Sources*, 2006, 159, 111.

[4] H. Wang, D. Wu, L. Wei and B. Tang, *J. Phys. Chem. C*, 2014, 118, 13607.